Nanofabrication of subwavelength, binary, high-efficiency diffractive optical elements in GaAs

J. R. Wendt, G. A. Vawter, R. E. Smith, and M. E. Warren
Sandia National Laboratories, Albuquerque, New Mexico 87185-0603

(Received 2 July 1995; accepted 1 August 1995)

A single-etch-step process for the fabrication of high-efficiency diffractive optical elements is presented. The technique uses subwavelength surface relief structures to create a material with an effective index of refraction determined by the fill factor of the binary pattern. Fabrication is performed using electron beam lithography and reactive-ion-beam etching on bulk GaAs, but the process is applicable to any material for which well-controlled etches exist. In this work, we designed and fabricated a blazed transmission grating for operation at 975 nm. The blazed grating exhibits a diffraction efficiency into the first order of 85% of the transmitted power. © *1995 American Vacuum Society.*

I. INTRODUCTION

Modern optoelectronic systems often require lenses and other micro-optics for modifying light signals. For practical, cost effective integration of these optical elements, it is desirable that the fabrication process be compatible with conventional microelectronic processing. One component of this compatibility is that the process be planar. For greatest applicability, it is desirable that the process yields optics of precision and broad functionality. Examples of the latter include off-axis and multifocal spot lenses. Figure 1 shows a segment of an arbitrary refractive optic along with four analogous diffractive optical elements. Refractive optics, Fig. 1(a), can provide ideal phase profiles but are nonplanar and not easily fabricated on the micron scale. The Fresnel zone equivalent, Fig. 1(b), is planar, reducing the refractive phase profile to a modulo 2π stepped phase profile. Some progress has been made in demonstrating these structures[1] but the fabrication is challenging. Conventional, multilevel binary optics,[2] Fig. 1(c), are planar, but only approximate the smooth phase profile of the Fresnel zones and have the additional disadvantage of requiring multiple lithographic and etch steps with stringent alignment and etch depth tolerances. The gradient index structure, Fig. 1(d), is perfectly planar and provides the desired phase profile, but is practically unobtainable in this ideal form (on the micron scale).

Recent work has suggested a way to create an arbitrary gradient index material using binary surface relief structures with features smaller than the wavelength of light in the material.[3,4] Such a structure may be thought of as an artificial material with an effective index of refraction that can be tailored by varying the fill factor of the binary pattern. The change in fill factor may be accomplished by varying the duty cycle (pulse-width modulation), as represented in Fig. 1(e), or the period (pulse-position modulation) of the binary pattern. Subwavelength diffractive structures have significant advantages over conventional multilevel diffractive optics including fabrication using a single lithography and etch step, the ability to achieve very high efficiencies and arbitrary phase profiles, the formation of antireflection surfaces,[5] and the incorporation of polarization-dependent properties.[6] The main challenge in fabrication is achieving the required small feature dimensions. We desire to integrate these optical elements into the surfaces of semiconductor optoelectronic materials with operating wavelengths on the order of 1 μm, requiring feature sizes on the order of 100 nm. Reported attempts at fabricating pulse-width modulated structures include a metallic reflection grating[7] for operation at 10.6 μm and blazed transmission gratings in silicon[8] for operation at 1.55 μm and in fused quartz[9] for operation at 633 nm. Pulse-position modulation has been used to demonstrate a reflective binary Bragg-type multibeam splitter at 1.064 μm.[10] In this previous work, the demonstrated efficiencies are not as high and/or the demonstrated diffractive optics are not as ambitious (in terms of equivalent lens speed) as that reported here.

In this paper, we present our work on the nanofabrication of subwavelength, binary diffractive optical elements in GaAs. We demonstrate a blazed transmission grating whose dimensions closely match the design parameters and which exhibits very high efficiency.

II. DESIGN

We designed a blazed transmission grating for operation at 975 nm. We chose a grating period of 3.285 μm to give a significant first order diffraction angle (17.3°), corresponding to the outermost Fresnel zone of a moderately fast lens ($f/1.7$). The requirement that the line/space features making up one period of the blazed grating be subwavelength, constrained by practical fabrication limits, led to the choice of ten line/space pairs per period. Because the features are only slightly smaller than the wavelength of light in the material, the design calculations are based on rigorous coupled wave analysis.[11] The technique allowed use of optimization algorithms to arrive at a structure based on maximizing the power in the first diffracted order.[12] A unique feature of our design procedure is that we did not limit ourselves solely to either pulse-width or pulse-position modulation but rather, allowed both the width and spacing of the grating ribs to vary in order to yield the most practically realizable design. Furthermore, the dimensions and aspect ratios of the etched grooves and ribs were constrained to lie within our fabrication capabilities. Specifically, the minimum rib dimension

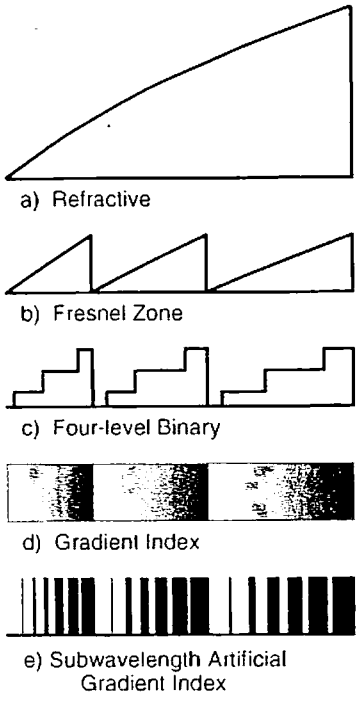

FIG. 1. Segment of an arbitrary refractive optical element and four analogous diffractive optical elements.

was set to 60 nm, the maximum rib aspect ratio was set to 10, the minimum groove width was set to 100 nm, and the maximum groove aspect ratio was set to 6. Without the flexible design and dimensional constraints, the most obvious design for a subwavelength blazed grating would be a linear variation in the duty cycle of a line/space pair resulting in vanishingly small rib widths at the low index end and vanishingly small grooves at the high index end [see Fig. 1(e)]. One period of the blazed grating design in this work is shown in Fig. 2. Note the nonlinear variation in rib and groove width across the pattern, for example, the minimum groove width occurs between the seventh and eighth ribs, not between the ninth and tenth as would be expected in a linear design. This design has a theoretical diffraction efficiency into the first order of over 98% of the transmitted power compared to 41% for a conventional two-level diffractive optic.

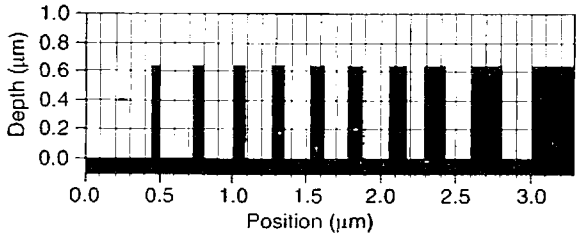

FIG. 2. Optimized line/space profile for one period of the blazed transmission grating. The narrowest line is 62.5 nm, the narrowest space is 115 nm, the etch depth is 642 nm, and the grating period is 3.285 μm.

III. FABRICATION

The stringent dimensional requirements of the above design were achieved using electron beam lithography and reactive-ion-beam etching (RIBE) with a Ni/SiO_2 mask. Fabrication was performed on a 3-in.-diam bulk GaAs wafer. The back side of the wafer was coated with an antireflection coating consisting of SiO_2/Nb_2O_5 layers to minimize the effect of reflections from the back side GaAs–air interface on the transmission measurements. The front side of the wafer was coated first with 110 nm of plasma-deposited SiO_2 and then spin coated with 210 nm of poly(methylmethacrylate) (PMMA) electron beam resist. Following electron beam patterning of the PMMA, 5 nm of chrome (for adhesion) and 60 nm of nickel were evaporated onto the sample and the unwanted metal lifted off. The Cr/Ni pattern was transferred first into the SiO_2 layer by reactive-ion etching (RIE) and then into the GaAs surface by RIBE. The fabrication steps are described in more detail below.

The electron beam lithography was performed on a JEOL JBX-5FE field emission system operating at 50 kV. A beam current of 500 pA, with a corresponding beam diameter of 6 nm, was used. The addressed pixel spacing was 5 nm in an 80 μm field. The PMMA thickness of 210 nm was chosen to be as thin as possible for maximum resolution while still allowing for clean, reliable lift off of the 65 nm evaporated Cr/Ni layer. The sub-tenth micron resolution required for the blazed grating is well within the capability of the JEOL instrument operated under the given conditions. The challenge of this work was to achieve the design dimensions etched in GaAs which required compensating for the proximity effect during exposure, resist deformation during metal evaporation, and any lateral dimension changes while transferring the Cr/Ni pattern to the SiO_2 and GaAs. Because the patterns are periodic on a scale less than the backscattered electron range (~4 μm at 50 kV), the proximity effect is expected to contribute a relatively uniform background dose across the pattern. This suggests that the proximity effect can be largely compensated using a single, optimized dose with an appropriately biased pattern. Pattern distortion was found to occur during the electron beam evaporation of the Cr/Ni etch mask and is attributed to deformation of the PMMA resist primarily caused by stress in the Cr/Ni film deposited on top of the PMMA. The PMMA pulls away at the top of the developed gap resulting in an increase in linewidth. It should be noted that this effect was minimized as much as possible by using a large source to sample distance of 27 in. and that the absolute magnitude of the effect is very small (≤50 nm). Because the etch depths required in this work are relatively shallow, and the etch mask relatively robust, no appreciable lateral dimension change was observed during either the SiO_2 RIE or the GaAs RIBE, as measured near the tops of the etched features.

The blazed grating pattern was biased using a manual procedure. Since we did not believe that formal proximity effect correction was necessary and had no *a priori* knowledge of the magnitude of the resist deformation effect, the blazed pattern was initially exposed unbiased relative to the design dimensions with the exception of a standard one-half pixel spacing (2.5 nm) resize to compensate for the finite

beam diameter. The pattern was exposed over a range of doses and developed for 1 min in a 1:3 solution of methyl isobutyl ketone (MIBK) and isopropyl alcohol (IPA). At the best apparent dose for the pattern, a region of the developed PMMA pattern was inspected, uncoated, at low voltage in a scanning electron microscope (SEM) and the line/space dimensions were measured. The rest of the wafer underwent Cr/Ni evaporation and liftoff and the line/space dimensions again were measured. Relative to the design dimensions, the developed PMMA pattern exhibited from 20 to 55 nm of increased linewidth across the pattern, and the lifted-off Cr/Ni lines exhibited an additional increase of from 5 to 45 nm. Fortunately, the proximity effect is greatest where the blazed pattern is densest while the resist deformation effect is greatest where the pattern is least dense (and hence more area of PMMA to stress and deform) so that these two effects combined to produce an amazingly uniform increase in final linewidth of 65±5 nm across the blazed grating. Of course, one cannot very well bias the smallest lines (e.g., 62.5 nm) downwards by 65 nm so a simple empirical rule was invented and employed. For linewidth design dimensions less than twice the average pattern increase (~130 nm), the pattern bias was one-half the pattern design dimension. For the larger linewidth design dimensions, the pattern bias was simply the pattern increase for that line (~65 nm).

The biased pattern was then exposed over a new, higher dose range based on the results of the first exposure. The PMMA and Cr/Ni linewidths were again measured at the best apparent dose. The pattern accuracy showed significant improvement with the average magnitude error in the blazed grating linewidth being less than 10 nm, although covering an absolute range from +13 to −20 nm. A second, minor pattern bias was then performed to make the linewidth errors as small and uniform as possible. It should be noted that these changes were smaller (~10 nm) than the expected run-to-run process variations and did not result in significant changes in measured performance.

The overall blazed grating pattern was written as a strip 80 μm high and 960 μm long. The height corresponds to a single writing field of the JEOL instrument so that no field stitches are present in that direction across the pattern. The best dose range for the blazed grating was found to be 500–550 $\mu C/cm^2$. After the Cr/Ni lift off, the SiO_2 layer was etched using CHF_3/O_2 RIE. For the relatively shallow etch depths used in this work, the SiO_2 layer serves primarily to facilitate removal of the Cr/Ni layer at the end of the fabrication sequence. For deeper etches, the SiO_2 would serve to extend the robustness of the etch mask. The GaAs was etched in a custom-built RIBE system with an electron cyclotron resonance (ECR) ion source. The etch gas was chlorine at a pressure of 2.5×10^{-4} Torr. The typical acceleration voltage and beam current densities were 300 eV and 0.62 mA/cm^2, respectively. Etches were performed on a timed basis according to system calibration and accounting for etch lag effects.[13] A scanning electron micrograph of the cross section of a fabricated blazed grating is shown in Fig. 3. The minimum feature size is 70 nm and the maximum aspect ratio is 10:1. As expected, there is etch depth variation across the pattern as a function of the etched groove width. The

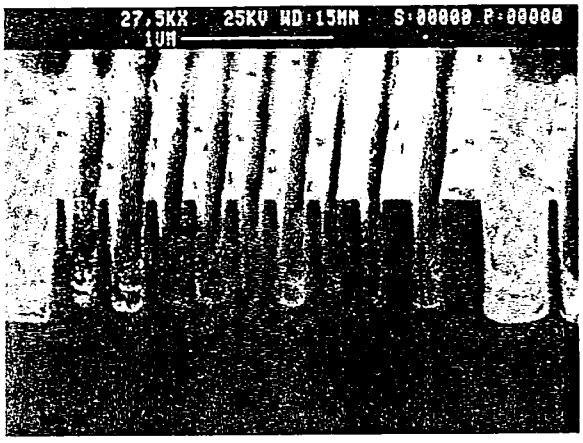

FIG. 3. Scanning electron micrograph of the cross section of a single period of the fabricated blazed transmission grating.

average etch depth is 705 nm, close to the design depth of 642 nm. The variation in etch depth is ±17.7% relative to the average etch depth. This is a significant variation but two things should be noted. One, because these are subwavelength structures where the effective index as a function of position is related to the integrated average of the index over a small volume of the structure at a given position, the exact geometry of the subwavelength features is not important so long as the effective index profile matches the design. Two, the etch depth variation could be parameterized and included in the design algorithm to compensate for the effect.

IV. EXPERIMENTAL RESULTS

The diffraction efficiency of the blazed grating was measured by two techniques. In both techniques, the incident laser light polarization was parallel to the grating lines and a reference detector was used to normalize out laser fluctuations. Light transmission was limited to the grating region by depositing a chrome slit aperture aligned precisely to the grating area (the grating lines are perpendicular to the slit). The relative power in the different transmitted diffracted orders was measured by scanning a detector with a slit aperture in a 180° arc about the grating aperture. The resulting profile of the diffracted orders is shown in Fig. 4. The integrated area under a given peak compared to the total integrated area for all peaks provides a measure of the diffraction efficiency of the grating into the given order. By this technique, the diffraction efficiency into the first order is 87% of the transmitted power. A second, more accurate measurement of diffraction efficiency into the first order was made using an integrating sphere. The total power in the first order was measured by positioning the integrating sphere at the first order diffracted angle (17.3°) and comparing that power to the total power transmitted through the grating as measured by positioning the integrating sphere as close to the grating aperture as possible. The diffraction efficiency into the first order measured by this technique is 85%, very close to the result determined above and consistent with the scattering of a few percent of the light out of the plane of the grating aperture. The 13% shortfall in measured efficiency compared

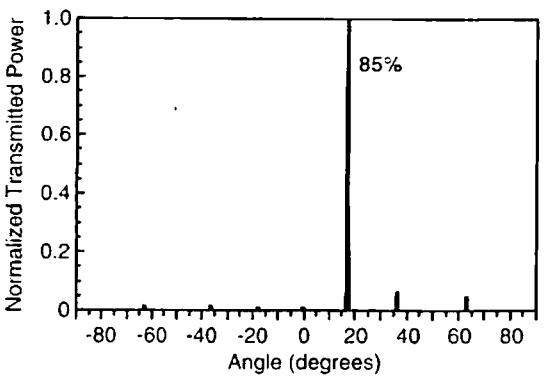

FIG. 4. Angular scan of the transmitted diffracted orders of the blazed grating. The measured diffraction efficiency into the first order is 85% of the transmitted power.

to the predicted theoretical efficiency is attributed to deviations in the line/space dimensions and etch depths of the fabricated grating compared to the design values. This result demonstrates the potential for fast ($f/1.7$), high-efficiency diffractive optical elements in the 1 μm wavelength region suitable for integration with optoelectronic devices.

V. SUMMARY

The nanofabrication of subwavelength, binary, high-efficiency diffractive optical elements has been demonstrated in GaAs utilizing electron beam lithography and reactive-ion-beam etching. A unique design procedure was used that employed both pulse-width and pulse-position modulation yielding a more practically realizable design. Successful fabrication of these structures was aided by constraining the design algorithm to dimensions and aspect ratios which were within the limits of our fabrication capabilities. The design dimensions were biased in the exposed pattern to result in final etched structures typically within 20 nm of the design values. The blazed transmission grating exhibited a diffraction efficiency into the first order of 85% of the transmitted power. This work demonstrates the potential for high-speed, high-efficiency lenses and other micro-optic elements fabricated in a single etch step and integrated with optoelectronic devices.

ACKNOWLEDGMENTS

The authors thank T. R. Carter and S. Samora for expert technical assistance. This work was performed at Sandia National Laboratories which is supported by the U.S. Department of Energy under Contract No. DE-AC04-94AL85000.

[1] G. J. Swanson and W. B. Veldkamp, Opt. Eng. 28, 605 (1989).
[2] P. D. Maker and R. E. Muller, J. Vac. Sci. Technol. B 10, 2516 (1992).
[3] W. Stork, N. Streibl, H. Haidner, and P. Kipfer, Opt. Lett. 16, 1921 (1991).
[4] M. W. Farn, Appl. Opt. 31, 4453 (1992).
[5] R. C. Enger and S. K. Case, Appl. Opt. 22, 3220 (1983).
[6] D. C. Flanders, Appl. Phys. Lett. 42, 492 (1983).
[7] M. Collischon, H. Haidner, P. Kipfer, A. Lang, J. T. Sheridan, J. Schwider, N. Streibl, and J. Lindolf, Appl. Opt. 33, 3572 (1994).
[8] Z. J. Zhou and T. J. Drabik, J. Opt. Soc. Am. A 12, 1104 (1995).
[9] F. T. Chen and H. G. Craighead, Opt. Lett. 20, 121 (1995).
[10] J. Turunen, P. Blair, J. M. Miller, M. R. Taghizadeh, and E. Noponen, Opt. Lett. 18, 1022 (1993).
[11] M. G. Moharam and T. K. Gaylord, J. Opt. Soc. Am. 72, 1385 (1982).
[12] M. E. Warren, R. E. Smith, G. A. Vawter, and J. R. Wendt, Opt. Lett. 20, 1441 (1995).
[13] R. A. Gottscho, C. W. Jurgensen, and D. J. Vitkavage, J. Vac. Sci. Technol. B 10, 2133 (1992).